HHS Public Access

Author manuscript

Oncogene. Author manuscript; available in PMC 2015 September 05.

Published in final edited form as:

Oncogene. 2015 March 5; 34(10): 1300–1311. doi:10.1038/onc.2014.64.

PDZ and LIM domain protein 1(PDLIM1)/CLP36 promotes breast cancer cell migration, invasion and metastasis through interaction with α-actinin

Zhongmin Liu[1], **Yun Zhan**[3], **Yizeng Tu**[1], **Ka Chen**[1], **Zhihua Liu**[3], and **Chuanyue Wu**[1,2,*]

[1]Department of Pathology, University of Pittsburgh School of Medicine, Pittsburgh, PA 15261, USA

[2]University of Pittsburgh Cancer Institute, Pittsburgh, PA 15213, USA

[3]State Key Laboratory of Molecular Oncology, Cancer Institute and Hospital, Chinese Academy of Medical Sciences and Peking Union Medical College, Beijing, China

Abstract

Increased CLP36 expression has been found to be closely associated with breast cancer progression. However, whether and how it contributes to malignant behavior of breast cancer cells were not known. We show here that CLP36 is critical for promoting breast cancer cell migration and invasion in vitro and metastasis in vivo, whereas it is dispensable for breast cell proliferation and anchorage independent growth in vitro and tumor growth in vivo. CLP36 interacted with both α-actinin-1 and -4 in breast cancer cells. Depletion of either α-actinin-1 or -4 inhibited breast cancer cell migration. Furthermore, mutations inhibiting the α-actinin-binding activity abolished the ability of CLP36 to promote breast cancer cell migration. Finally, depletion of CLP36 or disruption of the CLP36-α-actinin complex in breast cancer cells substantially inhibited Cdc42 activation, cell polarization and migration. Our results identify CLP36 as an important regulator of breast cancer cell migration and metastasis, and shed light on how increased CLP36 expression contributes to progression of breast cancer.

Keywords

CLP36; α-actinin; Breast cancer; Cell migration; Invasion; Metastasis

Introduction

Progression of cancer is associated with dramatic changes of its proteome. Determination of the proteomic changes, in particular those driving the progression and metastatic dissemination of cancer, is of paramount importance for diagnostics and treatment of cancer.

*Address correspondence to Dr. Chuanyue Wu, 707B Scaife Hall, Department of Pathology, University of Pittsburgh School of Medicine, 3550 Terrace Street, Pittsburgh, PA 15261, USA, Tel.: (412) 648-2350; Fax: (509) 561-4062; carywu@pitt.edu.

Conflict of interest

The authors declare no conflict of interest.

Recently, Pitteri and co-workers utilized an inducible HER2/neu mouse model of breast cancer (MMTV-rtTA/TetO-NeuNT mice), which synchronously develop invasive mammary carcinomas that recapitulate the morphologic, pathologic, and molecular features of ErbB2-positive human breast cancer [1], to characterize proteomic changes during breast cancer progression [2]. These studies have led to the identification of proteins whose expression is closely correlated with the progression of breast cancer. One of the proteins whose expression is dramatically increased in breast cancer cell progression is CLP36 [2] (also known as PDLIM1, Elfin or CLIM1[3, 4]), a member of the PDZ and LIM protein family that interacts with α-actinin[4–10]. The functional significance of the increase of CLP36 expression, however, remained to be determined.

The human α-actinin family comprises of four structurally related proteins, namely non-muscle α-actinin-1 and -4 and muscle α-actinin-2 and -3. α-actinin-4 was discovered based on its association with cell motility and cancer invasion [11]. Clinical studies of human patients with breast cancer have shown that increased cytoplasmic localization of α-actinin-4 was closely associated with an infiltrative histological phenotype and correlated significantly with a poorer prognosis [11]. Furthermore, a strong association of increased actinin-4 expression with advanced and metastatic cancers has also been demonstrated in other organs including colon, pancreas, ovarian and brain [12–15]. Experimentally, by directly manipulating α-actinin-4 expression in cells, several groups have demonstrated that α-actinin-4 promotes cell migration [12, 13, 16]. These findings, together with previous studies by us and others showing that CLP36 and actinin-4 co-localize and form a complex in cytoplasm [5, 9], prompted us to test whether increased CLP36 expression contributes to invasive and metastatic behavior of breast cancer. To do this, we suppressed CLP36 expression in breast cancer cells and found that it impaired their motility and invasiveness in vitro and metastasis potential in vivo, whereas the rate of proliferation, anchorage independent growth and tumor growth were not significantly altered. Mechanistically, we show that CLP36 can interact with both α-actinin-1 and -4 in breast cancer cells, and depletion of either CLP36 or α-actinin-1 or -4 was sufficient to inhibit breast cancer cell migration. Finally, to gain further mechanistic insights, we disrupted the CLP36-actinin complex and determined the consequences on key signaling pathways that are pertinent to cell migration and invasion. Our studies identify CLP36 as an important promoting factor for breast cancer cell invasion and metastasis, and shed light on how increased CLP36 expression contributes to progression of breast cancer.

Results

CLP36 is critical for breast cancer cell migration and invasion but is dispensable for cell proliferation

To begin to test the role of CLP36 in regulation of breast cancer behavior, we transfected MDA-MB-231 breast cancer cells with two different CLP36 siRNAs. Western blotting showed that CLP36 expression was dramatically reduced in CLP36 siRNA transfectants (Fig. 1A, lanes 2 and 3) compared with that in control transfectants (Fig. 1A, lane 1). Inhibition of CLP36 expression significantly reduced both the haptotactic migration (Fig. 1B) and random migration (Fig. 1C) of breast cancer cells. Similarly, depletion of CLP36

significantly inhibited breast cancer cell invasion (Fig. 1D). However, depletion of CLP36 did not significantly inhibit breast cancer cell adhesion to fibronectin (Fig. 1E) or proliferation (Fig. 1F). Furthermore, CLP36 deficient breast cancer cells were able to grow in an anchorage independent manner at a rate that was similar to that of control cells (Fig. 1G). Finally, abundant clusters of vinculin (a marker of focal adhesions) and actin stress fibers were detected in both the control and CLP36 knockdown cells (Fig. 1H). These results suggest that CLP36 is critical for breast cancer cell migration and invasion, albeit it is not essential for breast cancer cell-fibronectin adhesion, actin stress fiber formation, proliferation and anchorage independent growth.

Depletion of CLP36 diminishes breast cancer metastasis potential

Cell migration and invasion are essential for metastatic dissemination of breast cancer. To test whether CLP36 influences metastasis in vivo, we generated two CLP36 short hairpin RNA (shRNA) lentiviral vectors and a control lentiviral vector (shControl). The two CLP36 shRNAs (shCLP36-1 and shCLP36-2) target the same sequences as the two CLP36 siRNAs (KD1 and KD2). MDA-MB-231-Luc breast cancer cells were infected with the lentiviral vectors and the CLP36 levels in the shCLP36-1, shCLP36-2 and shControl cells were analyzed by Western blotting. As expected, the expression of CLP36 was reduced in shCLP36-1 and shCLP36-2 cells (Fig. 2A). Next, we analyzed the metastasis potential of breast cancer cells expressing different levels of CLP36 *in vivo* and found that metastasis of the shCLP36-1 and shCLP36-2 groups was significantly suppressed compared with that of the shControl cells (Fig. 2B), which was confirmed by quantification of *in vivo* luciferase activity (Fig. 2C). In contrast to the inhibition of metastasis, depletion of CLP36 did not significantly reduce tumor growth *in vivo* (Fig. 2D). Thus, consistent with the reduction of cell migration and invasion but not proliferation and anchorage independent growth *in vitro* (Fig. 1), depletion of CLP36 diminishes the metastasis potential but not the growth of breast cancer cells *in vivo*.

CLP36 interacts with α-actinin-1 and -4 in breast cancer cells

We next investigated the molecular mechanism by which CLP36 regulates breast cancer migration and invasion. CLP36 and α-actinin were abundantly expressed and co-localized in the leading edge of breast cancer cells (Figs. 3A–3C). Furthermore, α-actinin was readily co-immunoprecipitated with CLP36 from these cells (Fig. 3D, lane 2). By contrast, no α-actinin was detected in immunoprecipitates obtained with antibodies recognizing PDLIM4/RIL (Fig. 3E, lane 2), which shares significant sequence homology with CLP36 [17]. Because breast cancer cells express both α-actinin-1 and -4 [11], we tested whether CLP36 can interact with both. To do this, we transfected MDA-MB-231 cells with vectors encoding FLAG-α-actinin-1 or -4, respectively. Similar levels of FLAG-α-actinin-1 and -4 were expressed in the transfectants (Fig. 3F, lanes 2 and 3). We immunoprecipitated CLP36 from the cell lysates and analyzed the immunoprecipitates by Western blotting. Using a chemiluminescent substrate (Immobilon™ Western blot Chemiluminescent HRP substrate, Millipore) FLAG-α-actinin-4 (Fig. 3F, lane 5) but not FLAG-α-actinin-1 (Fig. 3F, lane 6) was readily detected in the CLP36 immunoprecipitates. However, using a more sensitive chemiluminescent substrate (SuperSignal West Femto Maximum Sensitivity Substrate, Thermo Scientific), FLAG-α-actinin-1 was detected in CLP36 immunoprecipitates (Fig. 3G,

lane 5), albeit the amount was smaller than that of FLAG-α-actinin-4 (Fig. 3G, compare lane 5 with lane 6). To confirm that CLP36 binds endogenous α-actinin-1, we immunoprecipitated CLP36 from MDA-MB-231 cells and analyzed the samples with an antibody specific for α-actinin-1. The results showed that endogenous α-actinin-1 was co-immunoprecipitated with CLP36 (Fig. 3H). Thus, CLP36 interacts with α-actinin-1 as well as -4 in MDA-MB-231 cells, albeit the interaction with α-actinin-1 appears to be weaker than that with α-actinin-4.

To test whether α-actinin-1 is involved in breast cancer cell migration, we transfected MDA-MB-231 cells with siRNAs (A1-KD1 and A1-KD2) targeting α-actinin-1. Western blotting with the α-actinin-1 specific antibody showed that the level of α-actinin-1 in A1-KD1 and A1-KD2 cells was reduced (Fig. 3I, the top panel). Probing the same samples with an antibody recognizing both α-actinin-1 and -4, showed that the total level of α-actinin proteins was not marked reduced (Fig. 3I, middle panel), suggesting that α-actinin-1 probably represents a relatively small fraction of α-actinin proteins in these cells. Importantly, actinin-1 deficient cells migrated significantly slower than that of control cells (Fig. 3J). Previous studies have shown that α-actinin-4 is critical for cancer cell migration [12, 13, 16]. Thus, as a control we transfected the cells with an α-actinin-4 siRNA. The level of α-actinin proteins in the α-actinin-4 siRNA transfectants was reduced (Fig. 3I, compare lane 4 with lane 1 in the middle panel), albeit a substantial amount of α-actinin proteins remained probably due to the presence of α-actinin-1 as well as incomplete depletion of α-actinin-4. Consistent with the previous studies[12, 13, 16], knockdown of α-actinin-4 inhibited cell migration (Fig. 3J). Collectively, these results suggest that both α-actinin-1 and -4, like their binding partner CLP36, are critically involved in breast cancer cell migration.

CLP36 but not RIL promotes breast cancer cell migration

To begin to test whether CLP36 interaction with α-actinin is important for breast cancer cell migration, we overexpressed FLAG-tagged CLP36 and RIL, respectively (Fig. 4A, lanes 2 and 3). As expected, abundant α-actinin was detected in FLAG-CLP36 immunoprecipitates (Fig. 4C, lane 5). By contrast, a much smaller amount of α-actinin was detected in FLAG-RIL immunoprecipitates (Fig. 4C, compare lane 6 with lane 5), suggesting that α-actinin preferentially interacts with CLP36 in breast cancer cells. Consistent with a role of α-actinin-binding in breast cancer cell migration, overexpression of FLAG-CLP36 (which binds strongly to α-actinin), but not that of FLAG-RIL (which binds poorly to α-actinin), significantly enhanced cell migration (Fig. 4B). Neither overexpression of FLAG-CLP36 nor that of FLAG-RIL altered the rate of proliferation under adherent condition (Fig. 4D), albeit increased expression of FLAG-RIL, but not that of FLAG-CLP36, inhibited anchorage independent growth (Fig. 4E).

α-actinin-binding is critical for promotion of breast cancer cell migration

To confirm that the CLP-36-α-actinin interaction is involved in regulation of breast cancer cell migration, we sought to introduce mutations into α-actinin-binding sites in CLP36. Previous studies have shown that CLP36 PDZ domain is critical for α-actinin-binding [5, 18]. Thus, we deleted the PDZ domain and found that it indeed reduced the interaction of

CLP-36 with α-actinin (Fig. 5A, compare lane 8 with lane 6). Importantly, deletion of the α-actinin-binding PDZ domain abolished the ability of CLP36 to promote breast cancer cell migration (Fig. 5B), confirming that α-actinin-binding is essential in this process.

Previous studies using purified recombinant CLP36 and α-actinin proteins suggest that a 26-residue conserved sequence termed as ZASP-like motif (ZM), which is located between the PDZ and LIM domains, may constitute a second α-actinin-binding site [18]. We deleted ZM and found that it also abolished the ability of CLP36 to promote breast cancer cell migration (Fig. 5B). However, co-immunoprecipitation experiments showed that deletion of ZM did not obviously reduce the interaction of CLP-36 with α-actinin in breast cancer cells (Fig. 5A, lane 7), suggesting that α-actinin-binding, although necessary, probably is not sufficient for promoting breast cancer cell migration.

CLP36 regulates Cdc42 activation and cell polarity

To gain insights into the signaling pathways through which CLP36 influences breast cancer cell migration, we analyzed the effects of CLP36 deficiency on signaling intermediates that are pertinent to cell migration. The results showed that depletion of CLP36 significantly inhibited activation of Cdc42 (Fig. 6, A and B) but not that of Akt and ERK (Fig. 6C). Activation of Cdc42 is known to be critical for cell polarization [19], a key step in cell migration. Thus, we analyzed the effect of CLP36 deficiency on cell polarization. Consistent with the inhibitory effect on Cdc42 activation, depletion of CLP36 compromised cell polarization (Fig. 6, D and E).

CLP36 regulates Cdc42 activation, cell polarization, migration and invasion through partnering with α-actinin

We next tested whether CLP36 regulates Cdc42 activation, cell polarization, migration and invasion through interaction with α-actinin. To do this, we generated an adenovirus encoding a dominant negative form of CLP36 (FLAG-ΔLIM) that contains the N-terminal α-actinin binding site but lacks the C-terminal LIM domain. MDA-MB-231 cells were infected with the FLAG-ΔLIM adenovirus (Fig. 7A, lane 2) or β-gal adenovirus as a control (Fig. 7A, lane 1). As expected, α-actinin was co-immunoprecipitated with FLAG-ΔLIM (Fig. 7A, lane 4). While abundant α-actinin was co-immunoprecipitated with endogenous CLP36 in control cells (Fig. 7B, lane 3), barely any α-actinin was co-immunoprecipitated with endogenous CLP36 in FLAG-ΔLIM-overexpressing cells (Fig. 7B, lane 4), indicating that overexpression of FLAG-ΔLIM effectively disrupted the CLP36-α-actinin complex. Of note, while CLP36 was detected in both Triton X-100 soluble (Fig. 7C, lane 1) and insoluble (Fig. 7C, lane 3) fractions of control cells, CLP36 was detected in Triton X-100 soluble (Fig. 7C, lane 2) but not insoluble (Fig. 7C, lane 4) fractions of FLAG-ΔLIM-overexpressing cells, suggesting that the formation of the CLP36-α-actinin complex is critical for CLP36 association with Triton X-100 insoluble fraction. Importantly, disruption of the CLP36-α-actinin complex, like depletion of CLP36 (Fig. 1), inhibited breast cancer cell migration (Fig. 8A) and invasion (Fig. 8B). Furthermore, disruption of the CLP36-α-actinin complex, like depletion of CLP36 (Fig. 6), compromised cell polarization (Fig. 8, C and D) and Cdc42 activation (Fig. 8, E and F) but not cell proliferation (Fig. 8G) or anchorage independent growth (Fig. 8H). Thus, CLP36, through partnering with α-actinin, promotes Cdc42

activation, cell polarization, migration and invasion but not proliferation or anchorage independent growth.

CLP36 interaction with α-actinin is critical for BT549 breast cancer cell migration and invasion

To test whether CLP36 interacts with actinin-1 and -4 in other human breast cancer cells, we expressed FLAG-α-actinin-1 and -4, respectively, in BT549 breast cancer cells (Fig. 9A, lanes 1 and 2). Co-immunoprecipitation analyses showed that both α-actinin-1 and -4 were co-immunoprecipitated with CLP36 (Fig. 9A, lanes 4 and 5), indicating that CLP36 can interact with both in these cells. Similar to what we found with MDA-MB-231 cells, depletion of CLP36 (Fig. 9B) significantly reduced BT549 cell migration (Fig. 9C) and invasion (Fig. 9D). To test whether disruption of the CLP36-α-actinin complex inhibits the migration and invasion of BT549 cells, we overexpressed FLAG-ΔLIM in BT549 cells (Fig. 10A, lane 2). Overexpression of FLAG-ΔLIM, as expected, effectively disrupted the formation of the CLP36-α-actinin complex (Fig. 10B, compare lanes 3 and 4). Importantly, disruption of the CLP36-α-actinin complex in BT549 cells, like that in MDA-MB-231 cells, markedly inhibited cell migration (Fig. 10C) and invasion (Fig. 10D). Thus, CLP36, through its interaction with α-actinin, promotes BT549 breast cancer cell migration and invasion.

Discussion

Development of metastatic spread is the leading cause of mortality in patients with breast cancer. Despite the importance, however, the molecular alterations that are responsible for increased migration, invasion and consequently metastasis of breast cancer are not well understood. Recent proteomic studies using an inducible HER2/neu mouse model of breast cancer have begun to reveal molecular alterations that could potentially drive breast cancer progression [2]. In these studies, CLP36 expression was found to dramatically increase with breast cancer progression [2]. This finding is interesting, as studies by us and others have shown that CLP36 binds α-actinin-4 [5, 9], a protein that has also been associated with the progression and poor prognosis of breast cancer [11]. Despite the correlation, however, whether or not the increase of CLP36 expression is functionally involved in the progression of breast cancer remained to be determined. In this study, we have carried out a series of in vitro and in vivo experiments to address this question. Our results clearly demonstrate that the increase of CLP36 expression is an important driving force for breast cancer cell migration, invasion and metastasis.

In addition to identifying a critical role of CLP36 in promoting breast cancer cell migration and invasion, the current study sheds light on how CLP36 functions in these processes. We have first compared the functions and activities of CLP36 and RIL, which share considerable sequence similarity. Whereas CLP36 binds strongly to α-actinin and promotes breast cancer cell migration and invasion, RIL binds poorly to α-actinin and is unable to promote breast cancer cell migration and invasion. These findings provide initial evidence suggesting that α-actinin-binding might be critical for these processes. Using two different strategies (site-directed mutagenesis ablating α-actinin-binding and dominant negative inhibition of the CLP36-α-actinin complex), we show that complex formation of CLP36

with α-actinin is critical for promoting breast cancer cell migration and invasion. Because both α-actinin-1 and -4 can bind CLP36 and depletion of either α-actinin-1 or -4, like that of CLP36, inhibited cell migration, theoretically both α-actinin-1 and -4 can contribute to breast cancer cell migration. Previous clinic studies with human breast cancer patients have shown that increased expression of α-actinin-4 is closely associated with an infiltrative histological phenotype and correlated significantly with a poorer prognosis[11]. Thus, the CLP36-α-actinin-4 complex likely plays an important role for promoting cell migration during breast cancer progression. Given the fact that α-actinin-1 also functions in breast cancer cell migration, it will be interesting to determine whether increased level or activity of α-actinin-1 is also associated with breast cancer progression.

The third important finding of the current study is that the CLP36-α-actinin complex regulates cell polarization, a key step in cell migration and invasion. How does the CLP36-α-actinin complex influence cell polarization? CLP36 and α-actinin were highly concentrated and co-localized in the leading edges of breast cancer cells (Figs. 3A–3C). Furthermore, the formation of the CLP36-α-actinin complex is crucial for activation of Cdc42 (Figs. 6B and 8F), which is known to play a central role in control of cell polarity [19]. These results suggest that the CLP36-α-actinin complex likely influences breast cancer cell polarization through, at least in part, promoting Cdc42 activation. In this regard, it is worth noting that the expression and activation of Cdc42 in human breast tumors are elevated compared with those in normal breast tissues [20, 21]. Furthermore, Cdc42 activation is critical for breast cancer cell migration and invasion [22–24], and dominant negative inhibition of Cdc42 markedly suppressed metastasis of breast cancer cells in an animal model [25].

In summary, the studies described in this report have identified a novel CLP36-α-actinin-Cdc42 signaling axis that functions in promoting breast cancer cell migration, invasion and metastasis. These experimental studies provide functional and mechanistic insights into previously reported findings showing that the expression of CLP36, α-actinin-4 and Cdc42 is elevated in breast cancer, and suggest that therapeutic approaches targeting the CLP36-α-actinin-Cdc42 signaling axis may be an effective intervention strategy against metastatic spread of breast cancer.

Materials and Methods

Antibodies and other reagents

Mouse monoclonal antibodies recognizing both α-actinin-4 and -1 were prepared using a GST fusion protein containing α-actinin-4 residues 311–911 as an antigen based on our previously described method [26, 27]. The following antibodies were purchased: anti-CLP36 antibody (Imegenex); antibody recognizing α-actinin-1 but not -4 (Abnova); anti-FLAG M2 and anti-vinculin antibodies (Sigma); Phospho-Akt (Ser473) and Phospho-Erk1/2 (Thr202/Tyr204) antibodies (Santa Cruz Biotech); Akt and Erk1/2 antibodies (Cell Signaling); anti-GM130 antibody (BD biosciences); ™2-conjugated anti-Goat IgG (H+L) and RhodamineRed™-X-conjugated anti-mouse IgG(H+L) antibodies and horseradish peroxidase-conjugated antibodies (Jackson ImmunoResearch Laboratories, West Grove, PA). FITC-phalloidin was from Sigma. Chemiluminescent substrate was from Millipore

(Catalog number WBKLS0500). In some Western blotting experiments, a SuperSignal West Femto Maximum Sensitivity Substrate (Thermo Scientific product number 34096) was used.

RNA interference

The sequences targeted by CLP36 siRNAs were (A) 5′-GCAAGGCGGCTCTA-GCTAA-3′ (KD1) and (B) 5′-GCAGCCTTGTCATCGACAA-3′ (KD2). The sequences targeted by α-actinin-1 siRNAs were (A) 5′-CCAGACCTACCACGTCAATAT-3′(A1-KD1) and (B) 5′-CCATCATGACTTACGTGTCTA-3′(A1-KD2). The sequence targeted by α-actinin-4 siRNA was 5′-CATCGCTTCCTTCAAGGTCTT-3′ (A4-KD) [13]. Cells were transfected twice with the siRNAs or an irrelevant small RNA (5′-GAAUGCCGGCAGGCAUCUCTT-3′) as a control using Lipofectamine 2000 (Invitrogen). Two days after siRNA transfection, the cells were harvested and analyzed.

Lentivirus production and infection

The CLP36 shRNA shCLP36-1 or shCLP36-2 targeting the same sequence as CLP36 siRNAs KD1 or KD2 or an irrelevant hairpin RNA (5′-GAAUGCCGGCAGGCAUCUCTT-3′) was cloned into pSIH1 vector. The pSIH1-shControl, pSIH1-shCLP36-1 and pSIH1-shCLP36-2 recombinant lentiviruses were produced by co-transfection of HEK 293T cells with the shRNA lentivirus expression plasmids and packaging plasmids (PLP1/PLP2 and VSVG) using Lipofectamine 2000. Virus particles were harvested 48h after transfection. MDA-MB-231-Luc cells were infected with recombinant lentivirus-transducing units plus 5 μg/ml polybrene. Two days after infection, cells were treated with 1 mg/ml puromycin to select cells stably expressing the shRNAs.

Experimental metastasis

Experimental metastasis was analyzed at Cancer Institute and Hospital, Chinese Academy of Medical Sciences in Beijing, China (the protocols were approved by the Beijing Medical Experimental Animal Care Commission). Four to six weeks old female NOD/SCID mice were divided into three groups (shControl, shCLP36-1 and shCLP36-2), each of which consisted of 9 mice. Each mouse was injected with 6×10^5 cells in phosphate-buffered saline via tail vein. Ten weeks later, the mice were anaesthetized with barbital sodium (200 mg/kg, i.p.), and injected with D-luciferin (150mg/kg, i.p.) 15 minutes before imaging. Metastasis was determined using a Xenogen optical *in vivo* imaging system (IVIS Lumina, Caliper Life Sciences). Values of bioluminescence signal were measured, quantified and expressed as photon counts per area.

CLP36 expression vectors and transfection

To generate vectors encoding FLAG-tagged full length CLP36 (residues 1–329), ΔPDZ (residues 68–329), ΔZM(residues 1–137 and 164–329) or ΔLIM mutant (residues 1–250), the CLP36 cDNAs were cloned into pFLAG-CMV-6c (Sigma). Cells were transfected with the vectors using Lipofectamine 2000. One day after transfection, the cells were harvested and analyzed.

Adenoviral expression vector and infection

Adenoviral vectors encoding FLAG-ΔLIM was generated using the AdEasy system flowing a protocol that we described [28]. MDA-MB-231 or BT549 cells were infected with the adenoviruses and the infection efficiency was monitored by the expression of GFP encoded by the adenoviral vectors, which typically reached approximately 100% within 2 days. The infected cells were harvested and analyzed 2 days after infection.

Preparation of Triton X-100 soluble and insoluble Fractions

Total lysates were prepared by extraction of the cells with 1% SDS in PBS buffer (pH 7.4). Triton X-100 soluble and insoluble fractions were prepared as we described [29]. Briefly, cells were rinsed with PBS buffer, extracted with 1% Triton X-100 in PBS buffer (pH 7.4), and centrifuged at 20,800g at 4°C for 15 minutes. The supernatants (soluble fractions) and pellets (insoluble fractions) were collected. The pellets were then extracted with 1% SDS in PBS buffer.

Immunoprecipitation

To immunoprecipitate FLAG-tagged proteins, cells (as specified) were lysed with the lysis buffer (1% Triton X-100 in 1×PBS, pH 7.4, containing 2 mM Na_3VO_4, and protease inhibitors). The lysates were mixed with agarose beads conjugated with anti-FLAG antibody M2. To immunoprecipitate endogenous CLP36, cells were lysed as described above. The lysates were mixed with anti-CLP36 antibody, and then incubated with UltraLink Immobilized Protein G beads (Pierce). The beads were washed five times and the immunoprecipitates were analyzed by Western blotting.

Immunofluorescent staining

Cells were plated on fibronectin (10 μg/ml) coated cover slips and incubated at 37°C for 24 hours. The cells were then fixed with 4% paraformaldehyde, permeabilized with 0.1% Triton X-100 in 50 mM Tris·HCl (pH 7.4) containing 150 mM NaCl and 1 mg/ml BSA, and stained with antibodies or FITC-phalloidin as specified.

Cell proliferation

Cell proliferation was performed as described [30]. Briefly, cells were seeded at 5,000 per well in triplicate on 96-well plates in growth medium supplemented with 10% serum, and were cultured for various periods of time. Viable cells were quantified using a MTT assay (Invitrogen, Cat#M6494).

Soft agar colony formation assay

Anchorage-independent growth was measured as described [30]. Briefly, 0.5% agarose in growth medium was added to 35mm dishes and allowed to solidify. 10,000 cells/dish in 0.3% agarose solution were plated in triplicate and cultured for 2 weeks. At the end of incubation, colonies from four randomly selected microscopic fields (3.14 mm^2/field) were photographed. Colonies with diameter larger than 15 um in each field were quantified.

Tumor growth

Cell suspensions (6×10^5 cells/mouse) were mixed 1:1 with Matrigel and injected into the mammary fat pads of four to six weeks old female NOD/SCID mice. Thirty mice were used, in which ten mice were injected with each of the cell types (shCLP36-1, shCLP36-2 or shControl cells). Twelve weeks after injection, the mice were suffocated in CO_2 and the tumors were surgically removed and weighed.

Cell-ECM adhesion assay

Cell–ECM adhesion was performed as described [31]. Cells were labeled with Calcein-AM for 30 minutes and seeded (5×10^4 cells/well) in triplicates in fibronectin-coated 96-well plates. The fluorescence from total seeded cells was measured with a Fluorescence Reader (excitation wavelength=485 nm; emission wavelength=535 nm). The plates were centrifuged at 60.4 *g* for 3 minutes at 4°C to facilitate cell settlement. The plates were then centrifuged upside-down at 60.4 *g* for 15 seconds. After removing detached cells, the fluorescence from attached cells was measured. Cell adhesion was calculated as the fluorescence reading of attached cells divided by the fluorescence reading of total seeded cells.

Cdc42 activation assay

Cdc42 activity was determined using a colorimetric-based Cdc42 activity assay (G-LISA; Cytoskeleton, Denver, CO). Briefly, proteins were isolated with the lysis buffer, snap frozen, and processed following the manufacture's protocol. The samples (12.5 μg cell lysate/well) were added into wells containing the Cdc42-GTP-binding protein. Active Cdc42 was captured by the Cdc42-GTP-binding protein and detected with an anti-Cdc42 antibody. Total Cdc42 in the samples was detected by Western blotting with an antibody recognizing total Cdc42 and quantified using ImageJ. Cdc42 activation is expressed as the level of active Cdc42 after normalization for the amount of total cdc42.

Cell migration

Haptotactic cell migration was analyzed using Transwell motility chambers as we described [29]. Briefly, the undersurface of the membrane (8-mm pore size) of the Transwell motility chambers (Costar) was coated with 10 ug/ml fibronectin. Cells were added to the upper chambers (50,000 cells/chamber) and incubated at 37 °C for 3 hours. The cells on the upper surface of the membrane were removed. The cells on the undersurface were fixed and stained with 0.25% crystal violet. Cells from at least four randomly selected microscopic fields were quantified. A random cell migration assay was used in the experiments shown in Fig 1C, in which both sides of the membrane of the Transwell motility chambers were coated with 10 ug/ml fibronectin. Cell migration was analyzed as described above.

Cell invasion

Cell invasion was analyzed using Matrigel invasion chambers (Becton Dickinson) following the manufacturer's protocol. Briefly, cells were suspended in 0.2 ml of DMEM and added to the invasion chambers (50,000 cells/chamber), which were placed in wells of 24-well plates containing 0.75 ml/well of culture medium supplemented with 10% fetal bovine serum. The

cells were cultured for 24 hours and cells that remained on the upside of the filter were removed. The remaining cells were stained with 0.25% crystal violet. The cells from at least four randomly selected microscopic fields were counted.

Cell polarity

Cell polarity was analyzed using a Golgi reorientation assay as described [32]. Briefly, confluent monolayers of cells were wounded with a pipette tip. Cells were co-stained with anti-GM130 antibody and DAPI. To measure Golgi orientation, 120° angles were drawn from the center of the nucleus on cells that lined the edge of the wound, creating three sectors. The angles were drawn such that one of the 120° sectors faced the edge of the wound. All cells with Golgi in the sector facing the wound front were scored positive. Cells with Golgi encompassed a sector away from the wound edge or spanned any two or more sectors were considered negative and not scored. For each time point, at least 20 cells were examined. Data are expressed as means ± SE.

Statistic analysis

Student's *t* test was used for statistical analyses of the results. For analysis of metastasis in mice, Mann-Whitney U test was used to determine the *p* value by comparing photon counts per area. *P* values <0.05 were considered statistically significant.

Acknowledgments

This work was supported by NIH Grant GM65188 to C.W.

References

1. Cardiff RD, Anver MR, Gusterson BA, Hennighausen L, Jensen RA, Merino MJ, et al. The mammary pathology of genetically engineered mice: the consensus report and recommendations from the Annapolis meeting. Oncogene. 2000; 19:968–88. [PubMed: 10713680]
2. Pitteri SJ, Kelly-Spratt KS, Gurley KE, Kennedy J, Buson TB, Chin A, et al. Tumor microenvironment-derived proteins dominate the plasma proteome response during breast cancer induction and progression. Cancer Res. 2011; 71:5090–100. [PubMed: 21653680]
3. Kotaka M, Ngai SM, Garcia-Barcelo M, Tsui SK, Fung KP, Lee CY, et al. Characterization of the human 36-kDa carboxyl terminal LIM domain protein (hCLIM1). J Cell Biochem. 1999; 72:279–85. [PubMed: 10022510]
4. Bauer K, Kratzer M, Otte M, de Quintana KL, Hagmann J, Arnold GJ, et al. Human CLP36, a PDZ-domain and LIM-domain protein, binds to alpha-actinin-1 and associates with actin filaments and stress fibers in activated platelets and endothelial cells. Blood. 2000; 96:4236–45. [PubMed: 11110697]
5. Vallenius T, Luukko K, Makela TP. CLP-36 PDZ-LIM protein associates with nonmuscle alpha-actinin-1 and alpha-actinin-4. J Biol Chem. 2000; 275:11100–5. [PubMed: 10753915]
6. Kotaka M, Kostin S, Ngai S, Chan K, Lau Y, Lee SM, et al. Interaction of hCLIM1, an enigma family protein, with alpha-actinin 2. J Cell Biochem. 2000; 78:558–65. [PubMed: 10861853]
7. Vallenius T, Scharm B, Vesikansa A, Luukko K, Schafer R, Makela TP. The PDZ-LIM protein RIL modulates actin stress fiber turnover and enhances the association of alpha-actinin with F-actin. Exp Cell Res. 2004; 293:117–28. [PubMed: 14729062]
8. Tamura N, Ohno K, Katayama T, Kanayama N, Sato K. The PDZ-LIM protein CLP36 is required for actin stress fiber formation and focal adhesion assembly in BeWo cells. Biochem Biophys Res Commun. 2007; 364:589–94. [PubMed: 17964547]

9. Liu Z, Blattner SM, Tu Y, Tisherman R, Wang JH, Rastaldi MP, et al. Alpha-actinin-4 and CLP36 protein deficiencies contribute to podocyte defects in multiple human glomerulopathies. J Biol Chem. 2011; 286:30795–805. [PubMed: 21680739]
10. Miyazaki K, Ohno K, Tamura N, Sasaki T, Sato K. CLP36 and RIL recruit alpha-actinin-1 to stress fibers and differentially regulate stress fiber dynamics in F2408 fibroblasts. Exp Cell Res. 2012; 318:1716–25. [PubMed: 22659164]
11. Honda K, Yamada T, Endo R, Ino Y, Gotoh M, Tsuda H, et al. Actinin-4, a novel actin-bundling protein associated with cell motility and cancer invasion. J Cell Biol. 1998; 140:1383–93. [PubMed: 9508771]
12. Quick Q, Skalli O. Alpha-actinin 1 and alpha-actinin 4: contrasting roles in the survival, motility, and RhoA signaling of astrocytoma cells. Exp Cell Res. 2010; 316:1137–47. [PubMed: 20156433]
13. Honda K, Yamada T, Hayashida Y, Idogawa M, Sato S, Hasegawa F, et al. Actinin-4 increases cell motility and promotes lymph node metastasis of colorectal cancer. Gastroenterology. 2005; 128:51–62. [PubMed: 15633123]
14. Kikuchi S, Honda K, Tsuda H, Hiraoka N, Imoto I, Kosuge T, et al. Expression and gene amplification of actinin-4 in invasive ductal carcinoma of the pancreas. Clin Cancer Res. 2008; 14:5348–56. [PubMed: 18765526]
15. Yamamoto S, Tsuda H, Honda K, Onozato K, Takano M, Tamai S, et al. Actinin-4 gene amplification in ovarian cancer: a candidate oncogene associated with poor patient prognosis and tumor chemoresistance. Mod Pathol. 2009; 22:499–507. [PubMed: 19151661]
16. Shao H, Wang JH, Pollak MR, Wells A. alpha-actinin-4 is essential for maintaining the spreading, motility and contractility of fibroblasts. PLoS One. 2010; 5:e13921. [PubMed: 21085685]
17. Te Velthuis AJ, Isogai T, Gerrits L, Bagowski CP. Insights into the molecular evolution of the PDZ/LIM family and identification of a novel conserved protein motif. PLoS One. 2007; 2:e189. [PubMed: 17285143]
18. Klaavuniemi T, Kelloniemi A, Ylanne J. The ZASP-like motif in actinin-associated LIM protein is required for interaction with the alpha-actinin rod and for targeting to the muscle Z-line. J Biol Chem. 2004; 279:26402–10. [PubMed: 15084604]
19. Etienne-Manneville S. Cdc42--the centre of polarity. J Cell Sci. 2004; 117:1291–300. [PubMed: 15020669]
20. Fritz G, Brachetti C, Bahlmann F, Schmidt M, Kaina B. Rho GTPases in human breast tumours: expression and mutation analyses and correlation with clinical parameters. Br J Cancer. 2002; 87:635–44. [PubMed: 12237774]
21. Fritz G, Just I, Kaina B. Rho GTPases are over-expressed in human tumors. International Journal of Cancer. 1999; 81:682–687.
22. Johnson E, Seachrist DD, DeLeon-Rodriguez CM, Lozada KL, Miedler J, Abdul-Karim FW, et al. HER2/ErbB2-induced breast cancer cell migration and invasion require p120 catenin activation of Rac1 and Cdc42. J Biol Chem. 2010; 285:29491–501. [PubMed: 20595387]
23. Yamaguchi H, Lorenz M, Kempiak S, Sarmiento C, Coniglio S, Symons M, et al. Molecular mechanisms of invadopodium formation: the role of the N-WASP-Arp2/3 complex pathway and cofilin. J Cell Biol. 2005; 168:441–52. [PubMed: 15684033]
24. Pichot CS, Arvanitis C, Hartig SM, Jensen SA, Bechill J, Marzouk S, et al. Cdc42-Interacting Protein 4 Promotes Breast Cancer Cell Invasion and Formation of Invadopodia through Activation of N-WASp. Cancer Research. 2010; 70:8347–8356. [PubMed: 20940394]
25. Bouzahzah B, Albanese C, Ahmed F, Pixley F, Lisanti MP, Segall JD, et al. Rho family GTPases regulate mammary epithelium cell growth and metastasis through distinguishable pathways. Molecular Medicine. 2001; 7:816–830. [PubMed: 11844870]
26. Tu Y, Huang Y, Zhang Y, Hua Y, Wu C. A new focal adhesion protein that interacts with integrin-linked kinase and regulates cell adhesion and spreading. J Cell Biol. 2001; 153:585–98. [PubMed: 11331308]
27. Tu Y, Wu S, Shi X, Chen K, Wu C. Migfilin and mig-2 link focal adhesions to filamin and the actin cytoskeleton and function in cell shape modulation. Cell. 2003; 113:37–47. [PubMed: 12679033]

28. Shi X, Wu C. A suppressive role of mitogen inducible gene-2 in mesenchymal cancer cell invasion. Mol Cancer Res. 2008; 6:715–24. [PubMed: 18505917]

29. Zhang Y, Tu Y, Gkretsi V, Wu C. Migfilin interacts with vasodilator-stimulated phosphoprotein (VASP) and regulates VASP localization to cell-matrix adhesions and migration. J Biol Chem. 2006; 281:12397–407. [PubMed: 16531412]

30. Uehara N, Matsuoka Y, Tsubura A. Mesothelin promotes anchorage-independent growth and prevents anoikis via extracellular signal-regulated kinase signaling pathway in human breast cancer cells. Mol Cancer Res. 2008; 6:186–93. [PubMed: 18245228]

31. Shi X, Ma YQ, Tu Y, Chen K, Wu S, Fukuda K, et al. The MIG-2/Integrin Interaction Strengthens Cell-Matrix Adhesion and Modulates Cell Motility. J Biol Chem. 2007; 282:20455–66. [PubMed: 17513299]

32. Nobes CD, Hall A. Rho GTPases control polarity, protrusion, and adhesion during cell movement. J Cell Biol. 1999; 144:1235–44. [PubMed: 10087266]

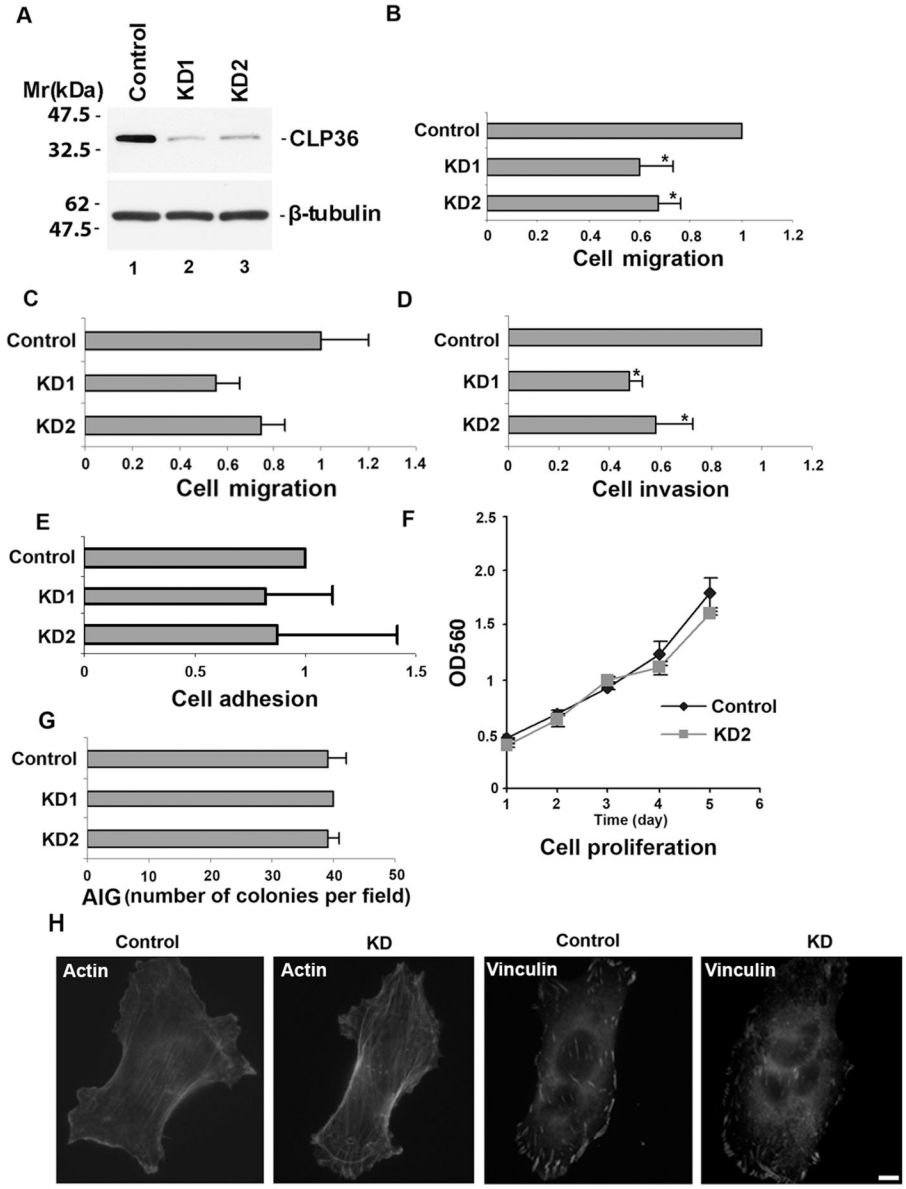

Figure 1. CLP36 is critical for breast cancer cell migration and invasion but not proliferation and anchorage independent growth

(A) Depletion of CLP36. MDA-MB-231 cells were transfected with CLP36 siRNA KD1, KD2 or a control siRNA. The cell lysates (6 μg proteins/lane) were analyzed by Western blotting with antibodies for CLP36 or tubulin (as a loading control). (B) Haptotactic cell migration was analyzed using Transwell motility chambers in which the undersurface of the membrane was coated with fibronectin. Migration of the KD1 and KD2 cells were compared to that of the control cells (normalized to 1). Bars represent means ± S.D. from three independent experiments. *$P < 0.05$ versus the control. (C) Random cell migration was analyzed using Transwell motility chambers in which both surfaces of the membrane were coated with fibronectin. Migration of the KD1 and KD2 cells were compared to that of the control cells (normalized to 1). The experiment was performed twice and similar results

were obtained. Panel C shows the results from a representative experiment (bars represent means ± S.D. from duplicate chambers). (D) Cell invasion was analyzed as described in the Materials and Methods. Invasion of the KD1 and KD2 cells were compared to that of the control cells (normalized to 1). Bars represent means ± S.D. from three independent experiments. *$P < 0.05$ versus the control. (E) Cell adhesion on fibronectin was analyzed as described in the Materials and Methods. Adhesion of the KD1 and KD2 cells were compared to those of the control cells (normalized to 1). Bars represent means ± S.D. from four independent experiments. (F) Anchorage-independent growth was analyzed as described in the Materials and Methods. The experiment was performed twice and similar results were obtained. Panel F shows the results from a representative experiment (bars represent means ± S.D. from triplicate dishes). (G) Cell proliferation was analyzed as described in the Materials and Methods. The experiment was performed twice and similar results were obtained. Panel G shows the results from a representative experiment (bars represent means ± S.D. from triplicate wells). (H) Control and CLP36 knockdown MDA-MB-231 cells were stained with a mouse anti-vinculin antibody and Rhodamine Red™-conjugated anti-mouse IgG antibodies. Actin filaments were detected with FITC-conjugated phalloidin. Bar, 10 μm. Because depletion of CLP36 did not significantly inhibit cell-fibronectin adhesion and depletion of CLP36 resulted in similar reductions of cell migration using either haptotactic or random migration assay, the assay for haptotactic migration, which is highly relevant to cancer cell invasion and metastasis, was used for cell migration experiments shown in other figures.

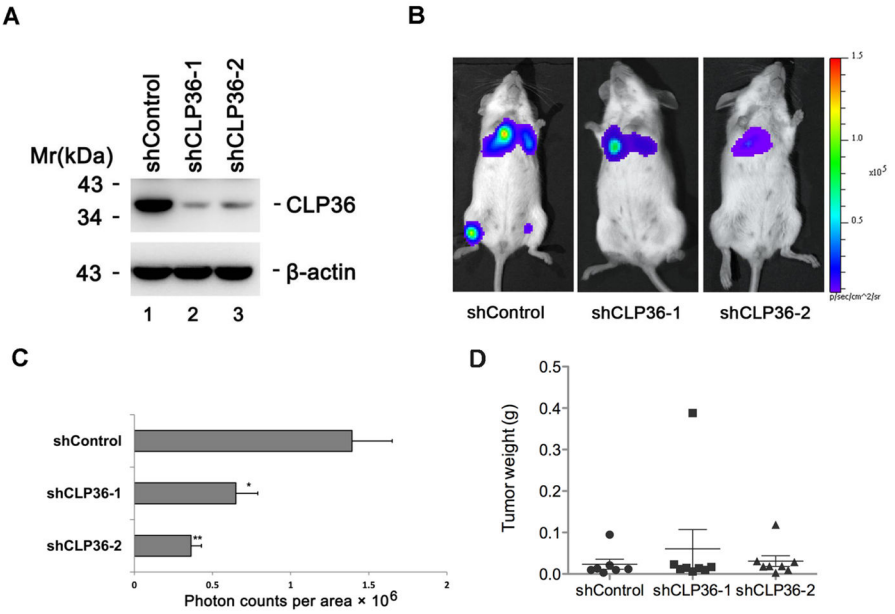

Figure 2. Depletion of CLP36 diminishes breast cancer metastasis potential

(A) MDA-MB-231-Luc cells were infected with shCLP36-1, shCLP36-2 or a control lentiviral vector. The cells were analyzed by Western blotting with antibodies recognizing CLP36 or β-actin (as a loading control). (B) The mice were divided into three groups (n=9 mice per group), 6×10^5 cells were injected into each mouse via tail vein. Ten weeks later, the mice were anaesthetized, and metastasis was determined using a Xenogen optical *in vivo* imaging system. Bioluminescence signals of a representative mouse from each group are shown. All images were obtained with the same settings (4 min exposure; photon signal: color scale from 9×10^4(min) to 1.5×10^5(max)). (C) Quantitative analysis of metastasis. The value of bioluminescence signals from each group were quantified and expressed as photon counts per area. Bars represent the values of each group (means ± S.D.). *P* values were obtained using Mann-Whitney U test. **P* < 0.05 and **p < 0.01 *versus* the control. (D) Tumor growth. In vivo tumorigenesis was assessed as described in the Matherials and Methods. shCLP36-1, shCLP36-2 or shControl cells (6×10^6 cells/mouse) were injected into the mammary fat pads of NOD/SCID mice (n=10 for each cell type). The tumors were removed and weighted twelve weeks after the mammary fat pad injection. Data represent means ±SEM.

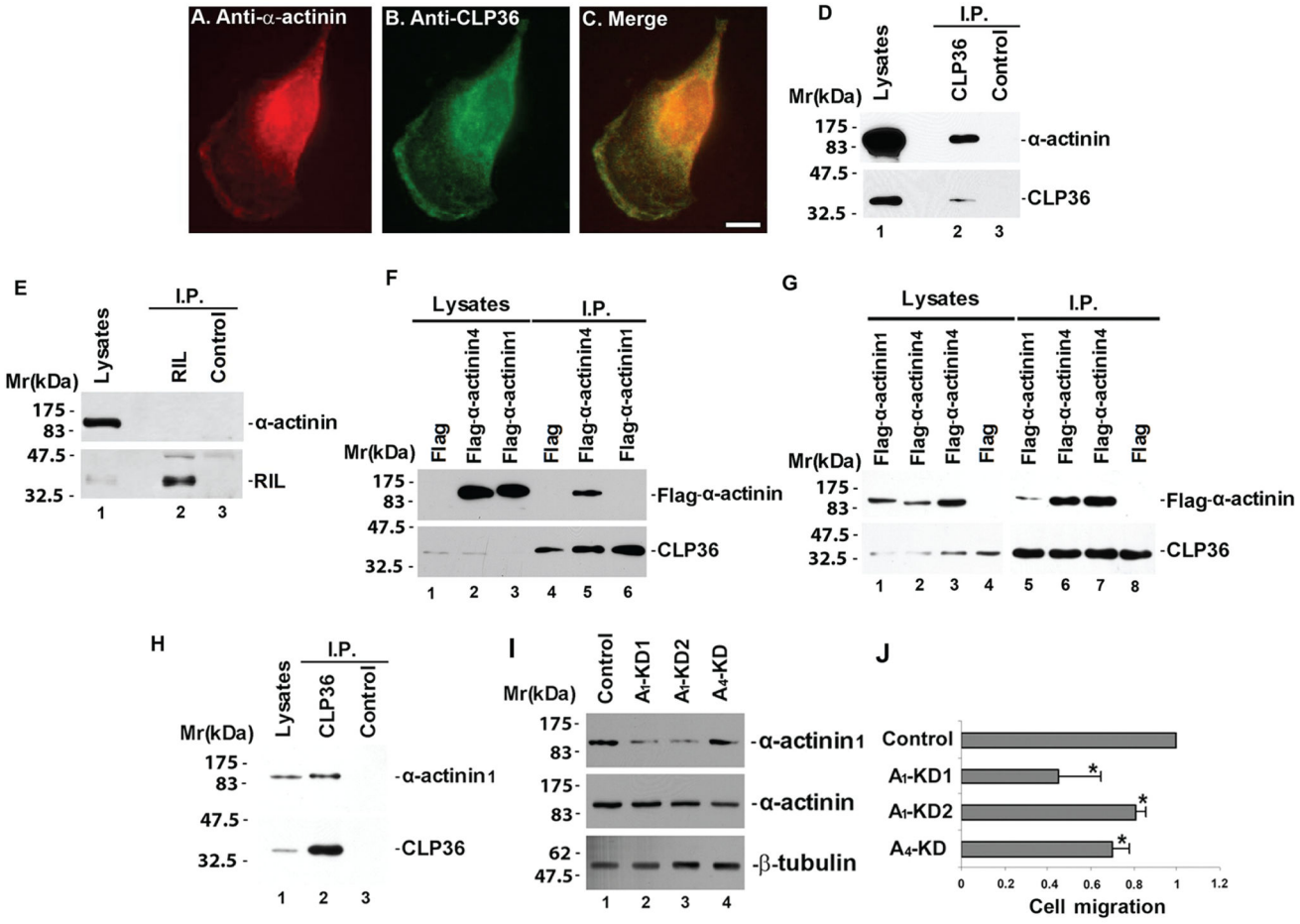

Figure 3. CLP36 interacts with α-actinin-1 and -4 in breast cancer cells

(A and B) MDA-MB-231 cells were dually stained with mouse anti-α-actinin antibody and goat anti-CLP36 antibody. The primary mouse and goat antibodies were detected with secondary Rhodamine Red™-conjugated anti-mouse IgG antibody and ™2-conjugated anti-goat IgG antibody, respectively. Bar, 10 μm. The immunofluorescent images were pseudo-colored and merged using NIH Image J program (C). (D) MDA-MB-231 cell lysates were mixed with an anti-CLP36 antibody or a control antibody that does not recognize CLP36. CLP36 and control immunoprecipitates were analyzed by Western blotting with anti-CLP36 and anti-α-actinin antibodies. (E) MDA-MB-231 cell lysates were mixed with an anti-RIL antibody or a control antibody that does not recognize RIL. RIL and control immunoprecipitates were analyzed by Western blotting with anti-RIL and anti-α-actinin antibodies. (F) Lysates of MDA-MB-231 cells transfected with FLAG, FLAG-α-actinin-1 or -4 were incubated with an anti-CLP36 antibody. Anti-CLP36 immunoprecipitates were analyzed by Western blotting with anti-CLP36 and anti-FLAG antibodies. (G) Lysates of MDA-MB-231 cells transfected with FLAG, FLAG-α-actinin-1 or FLAG-α-actinin-4 construct were incubated with an anti-CLP36 antibody. Anti-CLP36 immunoprecipitates were analyzed by Western blotting with anti-CLP36 and anti-FLAG antibodies and detected with an ultra-sensitive chemiluminescent substrate (Thermo Scientific product number 34096). The samples in lanes 2 and 6 were identical to those of lanes 3 and 7 except that the

cells were transfected with 25% less amount of the FLAG-α-actinin-4 construct (to ensure that the expression level of FLAG-α-actinin-4 was not higher than that of FLAG-α-actinin-1). (H) MDA-MB-231 cell lysates were mixed with an anti-CLP36 antibody or a control antibody that does not recognize CLP36. CLP36 and control immunoprecipitates were analyzed by Western blotting with anti-CLP36 and anti-α-actinin 1 antibodies. (I) α-actinin knockdown. MDA-MB-231 cells were transfected with α-actinin-1 siRNA (A1-KD1 or A1-KD2), α-actinin-4 siRNA A4-KD or a control small RNA. The cell lysates were analyzed by Western blotting with antibodies for α-actinin-1, α-actinin or tubulin (as a loading control) as indicated in the figure. (J) Haptotactic cell migration was analyzed as in Fig. 1B. Migration of the A1-KD1, A1-KD2 and A4-KD cells were compared to that of the control cells (normalized to 1). Bars represent means ± S.D. from three independent experiments. *$P < 0.05$ versus the control.

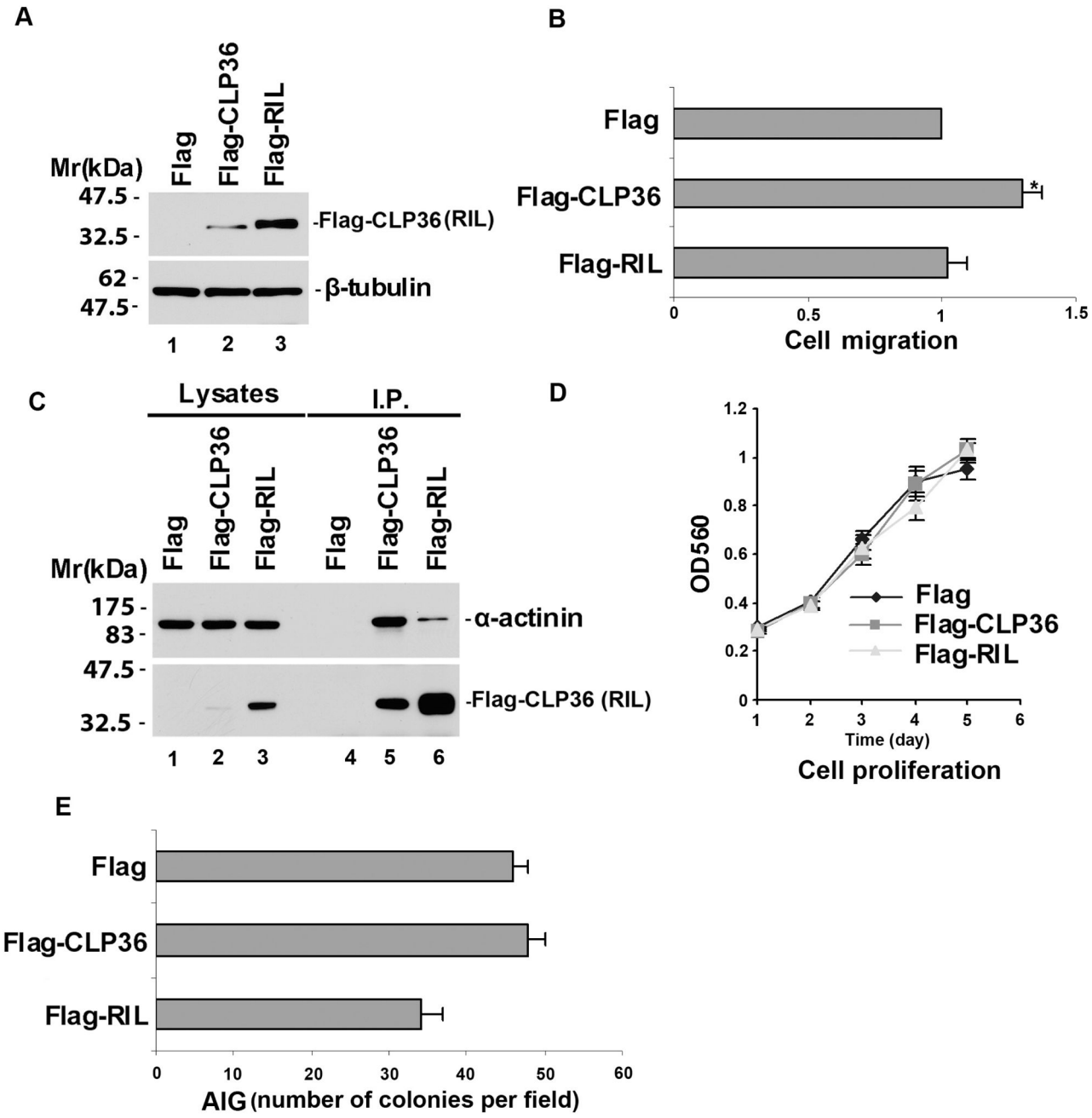

Figure 4. Overexpression of CLP36, but not that of RIL, promotes breast cancer cell migration

(A) FLAG-CLP36 and FLAG-RIL expression. Lysates (10 μg/lane) of MDA-MB-231 cells transfected with FLAG, FLAG-CLP36 or FLAG-RIL expression vector were analyzed by Western blotting with antibodies recognizing FLAG or tubulin (as a loading control). (B) Haptotactic cell migration was analyzed as in Fig. 1B. Migration of FLAG-CLP36 and FLAG-RIL expressing cells was compared to that of FLAG control cells (normalized to 1). Bars represent means ± S.D. from three independent experiments. **P* < 0.05 versus the control. (C) α-actinin interaction. FLAG-CLP36 or FLAG-RIL was immunoprecipitated from lysates of the cells transfected with FLAG, FLAG-CLP36 or FLAG-RIL vector with

M2 anti-FLAG antibody. The cell lysates (lanes 1–3) and immunoprecipitates (lanes 4–6) were analyzed by Western blotting with antibodies for α-actinin or FLAG as indicated. (D) Cell proliferation was analyzed as described in the Materials and Methods. The experiment was performed twice and similar results were obtained. Panel D shows the results from a representative experiment (bars represent means ± S.D. from triplicate wells). (E) Anchorage-independent growth was analyzed as described in the Materials and Methods. The experiment was performed twice and similar results were obtained. Panel E shows the results from a representative experiment (bars represent means ± S.D. from triplicate dishes).

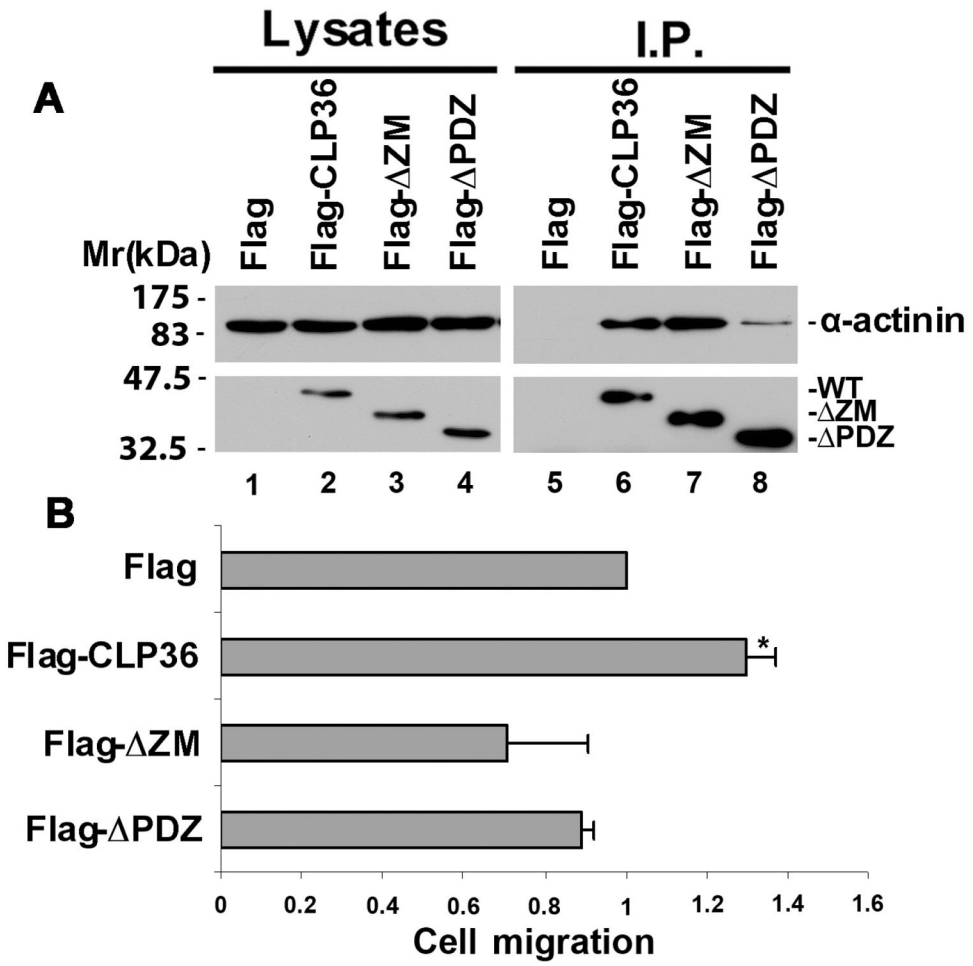

Figure 5. α-actinin binding is essential for CLP36-mediated promotion of breast cancer cell migration

(A) MDA-MB-231 cells transfected with FLAG, FLAG-CLP36, FLAG-ΔZM or FLAG-ΔPDZ were analyzed by immunoprecipitation with M2 anti-FLAG-antibody. The cell lysates (lanes 1–4) and anti-FLAG immunoprecipitates (lanes 5–8) were analyzed by Western blotting with antibodies for α-actinin or FLAG as indicated. (B) Haptotactic cell migration was analyzed as in Fig. 1B. Migration of FLAG-CLP36, FLAG-ΔZM and FLAG-ΔPDZ expressing cells was compared to that of FLAG control cells (normalized to 1). Bars represent means ± S.D. from three independent experiments. **P* < 0.05 versus the control.

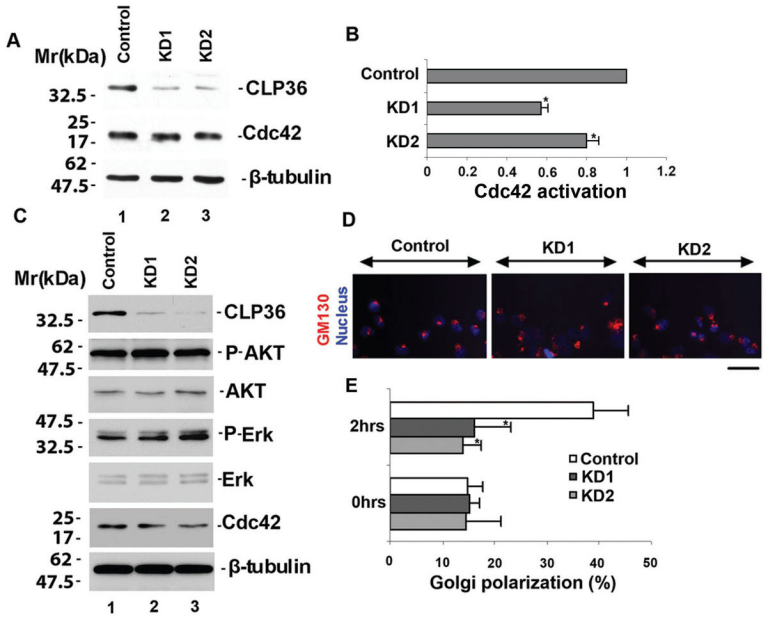

Figure 6. Depletion of CLP36 inhibits Cdc42 activation and cell polarization

(A) Lysates of the control and CLP36 knockdown cells were analyzed by Western blotting with antibodies recognizing CLP36, Cdc42 or tubulin (as a loading control) as indicated. (B) Cdc42 activation in control and CLP36 knockdown cells were analyzed as described in the Materials and Methods. Cdc42 activation in CLP36 knockdown cells was compared to that of control cells (normalized to 1). Bar represents mean ± S.D. from three independent experiments. *P < 0.05. (C) Lysates of the control and CLP36 knockdown cells were analyzed by Western blotting with antibodies recognizing CLP36, phospho-Akt (Ser473), Akt, phospho-Erk1/2 (Thr202/Tyr204), Erk1/2, Cdc42 or tubulin (as a loading control) as indicated. (D and E) Cell polarity. MDA-MB-231 cells transfected with control RNA or CLP36-specific siRNA were subjected to scratch wounding. The cells were stained for Golgi (GM130; red) and nuclei (DAPI; blue) (D). Bar, 10 μm. Cell polarity was analyzed as described in the Materials and Methods (E). Bars represent means ± S.D. from three independent experiments. *P < 0.05 versus the control.

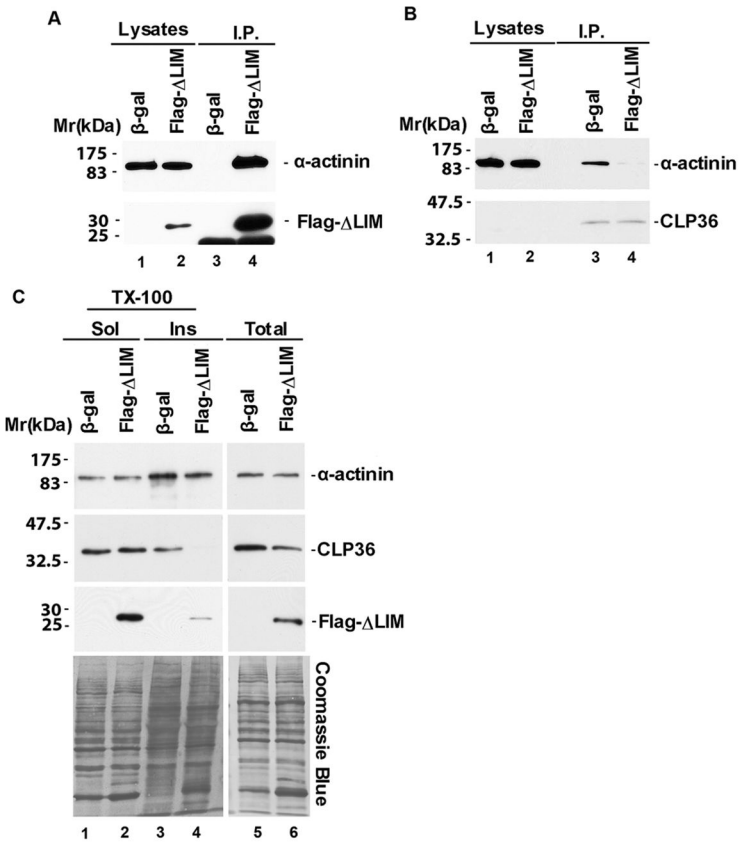

Figure 7. Dominant negative inhibition of the CLP36-α-actinin complex

(A) FLAG-ΔLIM expression and its binding to α-actinin. MDA-MB-231 cells were infected with adenoviral vectors encoding FLAG-ΔLIM or β-galactosidase (as a control). The cell lysates (lanes 1 and 2) and anti-FLAG immunoprecipitates (lanes 3 and 4) were analyzed by Western blotting with anti-FLAG or anti-α-actinin antibodies. (B) Inhibition of the CLP36-α-actinin complex. The cell lysates (lanes 1 and 2) and CLP36 immunoprecipitates (lanes 3 and 4) were analyzed by Western blotting with anti-α-actinin or anti-CLP36 antibodies. (C) The total lysates, Triton X-100 soluble and insoluble fractions of cells infected with adenoviral vectors encoding FLAG-ΔLIM or β-galactosidase were prepared as described in the Materials and Methods. The samples were analyzed by Western blotting with anti-α-actinin, anti-CLP36 or anti-FLAG antibodies and Coomassie blue staining as indicated.

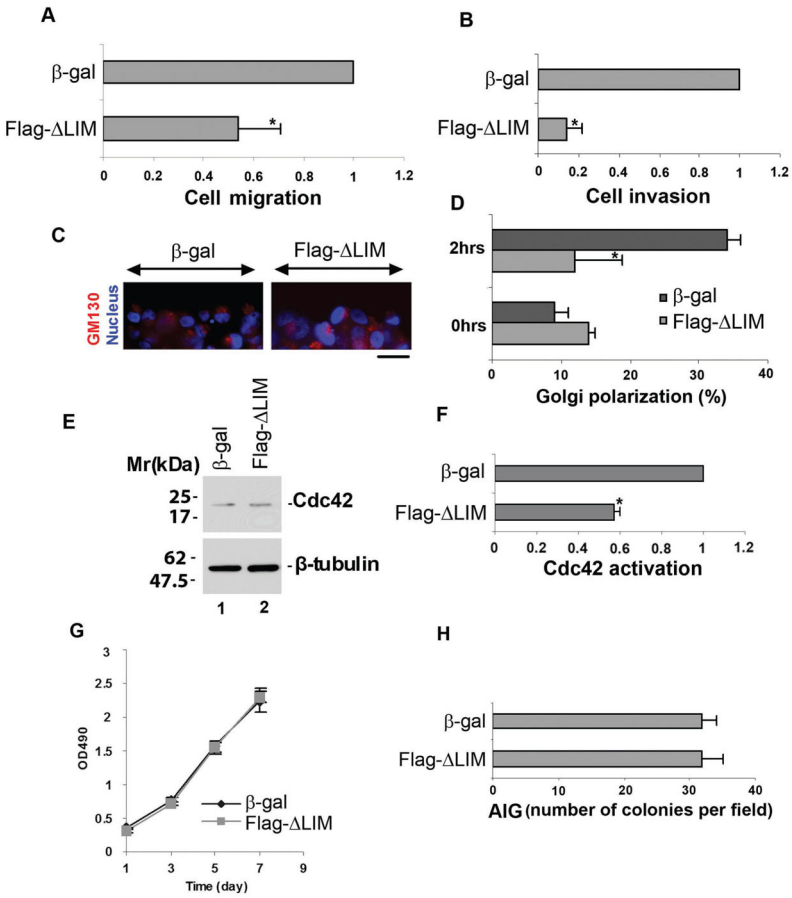

Figure 8. Disruption of the CLP36-α-actinin complex compromises Cdc42 activation, cell polarization, migration and invasion

(A and B) Cell migration and invasion. Haptotactic cell migration (A) and cell invasion (B) were analyzed as in Figs. 1B and 1D. Migration and invasion of FLAG-ΔLIM expressing cells were compared to those of β-gal control cells (normalized to 1). Bars represent means ± S.D. from three independent experiments. **P* < 0.05 versus the control. (C and D) Cell polarity. MDA-MB-231 cells infected with adenoviral vectors encoding FLAG-ΔLIM or β-galactosidase (as a control) were subjected to a scratch wounding. The cells were co-stained for Golgi (GM130; red) and nuclei (DAPI; blue) (C). Bar, 10 μm. Cell polarity was analyzed as described in the Materials and Methods (D). Bars represent means ± S.D. from three independent experiments. **P* < 0.05 versus the control. (E and F) Cdc42 activation. Lysates of Cdc42 MDA-MB-231 cells infected with adenoviral vectors encoding FLAG-ΔLIM or β-galactosidase (as a control) were analyzed by Western blotting with antibodies for Cdc42 and tubulin (as a loading control) (E). Active Cdc42 was quantified as described in the Materials and Methods (F). Cdc42 activation in FLAG-ΔLIM expressing cells was compared to that of control cells (normalized to 1). Bar represents mean ± S.D. from three independent experiments. *P < 0.05. (G) Cell proliferation was analyzed as described in the Materials and Methods. The experiment was performed twice and similar results were obtained. Panel G shows the results from a representative experiment (bars represent means ± S.D. from triplicate wells). (H) Anchorage-independent growth was analyzed as described

in the Materials and Methods. The experiment was performed twice and similar results were obtained. Panel H shows the results from a representative experiment (bars represent means ± S.D. from triplicate dishes).

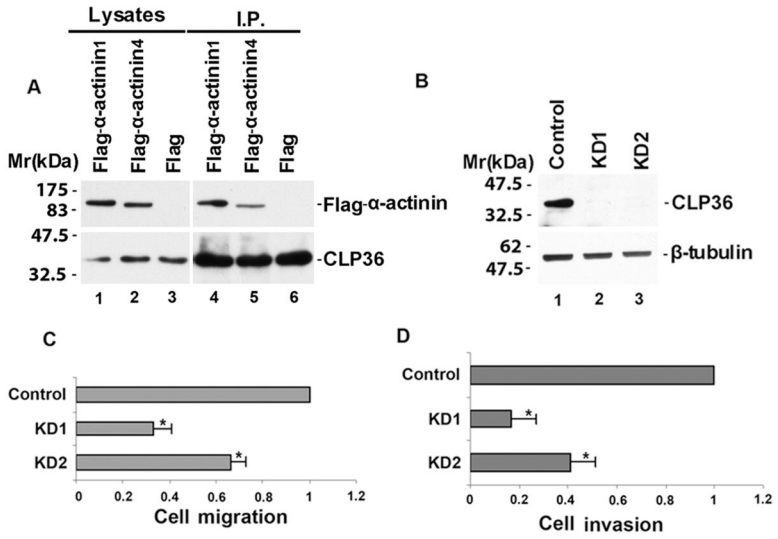

Figure 9. Depletion of CLP36 inhibits BT549 breast cancer cell migration and invasion

(A) Lysates of BT549 cells transfected with FLAG, FLAG-α-actinin-1 or -4 were incubated with an anti-CLP36 antibody. Anti-CLP36 immunoprecipitates were analyzed by Western blotting with anti-CLP36 and anti-FLAG antibodies. (B) Depletion of CLP36. BT549 cells were transfected with CLP36 siRNA KD1, KD2 or a control siRNA. The cell lysates (6 μg proteins/lane) were analyzed by Western blotting with antibodies for CLP36 or tubulin (as a loading control). (C and D) Haptotactic cell migration (C) and cell invasion (D) were analyzed as in Figs. 1B and 1D. Migration and invasion of the KD1 and KD2 cells were compared to those of the control cells (normalized to 1). Bars represent means ± S.D. from three independent experiments. **P* < 0.05 versus the control.

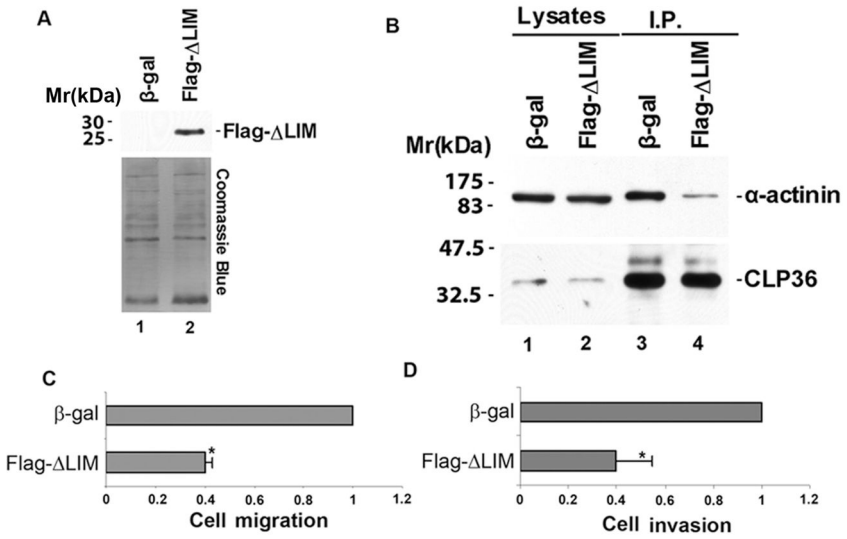

Figure 10. Disruption of the CLP36-α-actinin complex inhibits BT549 breast cancer cell migration and invasion

(A) FLAG-ΔLIM expression. BT549 cells were infected with adenoviral vectors encoding FLAG-ΔLIM or β-galactosidase (as a control) as described in the Materials and Methods. Cell lysates (lanes 1 and 2) were analyzed by Western blotting with anti-FLAG antibody and Coomassie blue staining as indicated. (B) Inhibition of the CLP36-α-actinin complex. The cell lysates (lanes 1 and 2) and CLP36 immunoprecipitates (lanes 3 and 4) were analyzed by Western blotting with anti-α-actinin or anti-CLP36 antibodies. (C and D) Cell migration and invasion. Haptotactic cell migration (C) and cell invasion (D) of FLAG-ΔLIM expressing cells were analyzed as in Figs. 1B and 1D and were compared to those of β-gal control cells (normalized to 1). Bars represent means ± S.D. from three independent experiments. **P* < 0.05 versus the control.